Pathologic and Molecular Heterogeneity in Imatinib-Stable or Imatinib-Responsive Gastrointestinal Stromal Tumors

Narasimhan P. Agaram,[1] Peter Besmer,[4] Grace C. Wong,[1] Tianhua Guo,[1] Nicholas D. Socci,[5] Robert G. Maki,[2] Diann DeSantis,[3] Murray F. Brennan,[3] Samuel Singer,[3] Ronald P. DeMatteo,[3] and Cristina R. Antonescu[1,4]

Abstract

Purpose: Gastrointestinal stromal tumor (GIST) is the most common sarcoma of the intestinal tract. Nearly all tumors express KIT protein, and most have an activating mutation in either *KIT* or *PDGFRA*. Therapy with selective tyrosine kinase inhibitors achieves a partial response or stable disease in ~80% of patients with advanced GIST. However, after an initial clinical response, some patients develop imatinib resistance. Our goal was to investigate the spectrum of pathologic response and molecular alterations in a group of GIST patients, clinically defined as having imatinib-stable/imatinib-responsive lesions, who underwent surgical resection.

Experimental Design: Forty-three tumor nodules from 28 patients were available for pathologic and molecular analysis, which included genotyping for primary and secondary *KIT*/*PDGFRA*-mutations, cell cycle alterations, and biochemical activation status of KIT and downstream targets. The transcriptional changes of a subset of these tumors were compared with a group of imatinib-naive GISTs on a U133A Affymetrix expression platform.

Results: The histologic response did not correlate with imatinib therapy duration or with proliferative activity. Second-site *KIT* mutation was identified in only one tumor nodule. Activation of KIT and downstream targets was consistent in all tumors analyzed. Ultrastructurally, a subset of tumors showed a smooth muscle phenotype, which correlated with overexpression of genes involved in muscle differentiation and function.

Conclusions: The histologic response to imatinib is heterogeneous and does not correlate well with clinical response. Second-site *KIT* mutations are rare in imatinib-responsive GISTs compared with imatinib-resistant tumors. The gene signature of imatinib-response in GISTs showed alterations of cell cycle control as well as up-regulation of genes involved in muscle differentiation and function.

Gastrointestinal stromal tumors (GIST) are KIT-expressing and KIT-signaling driven mesenchymal tumors, many of which have an activating mutation in either *KIT* or *PDGFRA*. Imatinib mesylate (Gleevec, Novartis Pharmaceuticals, Basel, Switzerland) inhibits the KIT and PDGFRA receptor tyrosine kinases and achieves partial responses or stable disease in nearly 80% of patients (1, 2). Although tyrosine kinase inhibitors have improved survival in advanced GIST, complete response is rare. Furthermore, it is now clear that the majority of patients who initially benefit from tyrosine kinase inhibitors eventually become resistant, with a median time to progression on imatinib mesylate of 2 years (3).

Responses to imatinib in GIST patients depend on the presence and genomic location of *KIT* mutations (4, 5). Patients with *KIT* exon 11 mutations have a partial response rate of 84% compared with a 0% partial response rate among patients without *KIT* mutations (4). The predominant mechanism of acquired resistance to imatinib is via additional mutations in *KIT* identified in half of the cases. Previously, we found that patients with acquired resistance due to a second-site *KIT* mutation had been on imatinib therapy longer (median = 27 months) than those without additional *KIT* mutation (14.5 months; ref. 6). The secondary mutations tend to be single amino acid substitutions in the KIT kinase domains and occur most often in exon 17. Second-site *KIT* mutations have thus far not been reported in nontreated tumors or tumors with primary resistance.

Clinical response to imatinib therapy is typically measured according to the conventional Southwest Oncology Group/Response Evaluation Criteria in Solid Tumors and is based on contrast-enhanced computed tomography or magnetic resonance imaging images (7). However, it is clear that these criteria are not ideal for identifying the development of drug resistance. In addition to size, the attenuation of a lesion, the presence of new lesions and/or sites of involvement, and nodules within any preexisting lesions are used to determine resistance (2, 8, 9). It is still debatable how accurately these imaging tools correlate with the biology of stable or responsive

Authors' Affiliations: Departments of [1]Pathology, [2]Medicine, and [3]Surgery, Memorial Sloan-Kettering Cancer Center; [4]Developmental Biology Program; and [5]Computational Biology Center, Sloan-Kettering Institute, New York, New York
Received 6/21/06; revised 9/12/06; accepted 10/6/06.

Grant support: ACS MRSG CCE-106841 (C.R. Antonescu), CA102774 (P. Besmer), HL/DK55748 (P. Besmer), PO1 CA 47179 (M.F. Brennan), and CA102613 (R.P. DeMatteo).

The costs of publication of this article were defrayed in part by the payment of page charges. This article must therefore be hereby marked *advertisement* in accordance with 18 U.S.C. Section 1734 solely to indicate this fact.

Requests for reprints: Cristina R. Antonescu, Department of Pathology, Memorial Sloan-Kettering Cancer Center, 1275 York Avenue, New York, NY 10021. Phone: 212-639-5721; Fax: 212-717-3203; E-mail: antonesc@mskcc.org.

doi:10.1158/1078-0432.CCR-06-1508

GIST lesions, and if they have the sensitivity to detect a subset of tumors or small region of a tumor that is undergoing subclinical progression. A further unresolved question relates to the heterogeneity of imatinib-stable lesions from a pathologic or molecular standpoint. It is not well established if clinical response or stable disease correlates with histologic response (fibrosis and necrosis) and/or quiescent growth and/or biochemical inhibition of KIT receptor signaling and downstream targets activity. In this study, we sought to investigate the spectrum of molecular and genomic changes in a group of clinically responsive or stable GISTs removed by elective surgery.

Materials and Methods

Clinicopathologic features. Patients with a diagnosis of GIST who were treated with imatinib and had a partial response or stable disease, based on contrast enhanced cross-sectional radiologic imaging, were identified from our prospective sarcoma database at Memorial Sloan-Kettering Cancer Center. Those who underwent elective surgical resection of their residual GIST tumors were selected for the study. Patients with focal resistance, defined as at least one nodule showing radiologic evidence of growth, were not included in the study. All patients were treated with imatinib mesylate (400-800 mg/d), which was discontinued 1 to 2 days before surgery. Clinical information was obtained from the database and review of medical charts, including extent of disease at the start of imatinib treatment, duration of imatinib therapy before surgical resection, and the best clinical response obtained on imatinib. This study was approved by the institutional review board.

The surgical specimen was reviewed, and the diagnosis of GIST was confirmed based on the histology and immunostaining for the KIT antibody. Histologic response to imatinib was assessed as a percentage and was graded, based on the gross and microscopic amounts of necrosis and fibrosis, using a previously proposed grading scheme (6): 1, minimal (0-10% response); 2, low (>10% and ≤50% response); 3, moderate (>50% and ≤90% response); and 4, high (>90% response). Other histologic variables, including the type of tumor (spindle/epithelioid) and mitotic count (per 50 high-power fields), were recorded.

KIT/PDGFRA *genotyping.* Mutation analysis was done as described previously (10). Genomic DNA was isolated from snap-frozen tumor tissue samples stored at −70°C, using a standard phenol/chloroform organic extraction protocol. Adequate DNA for mutational analysis was obtained in 43 tumor nodules from 28 patients. The genotype of patients 1 to 14 (Table 1) was previously reported (6). All cases were tested for the known sites of *KIT* (exons 9, 11, 13, 14, and 17) and *PDGFRA* (exons 12 and 18) mutations. One microgram of genomic DNA was subjected to PCR using Platinum TaqDNA Polymerase High Fidelity (Life Technologies, Inc., Gaithersburg, MD). Primer sequences and annealing temperatures were as described (10). In cases showing profound treatment effect, the mutational analysis was done in parallel from micro-dissected viable tumor areas on formalin-fixed, paraffin-embedded tissue. These areas were carefully selected to include mitotically active or viable areas with the highest Ki67 proliferation index to avoid false-negative results on frozen tissue secondary to necrosis. Direct sequencing of PCR products was done for all exons tested, and each ABI sequence was compared with the National Center for Biotechnology Information human *KIT* and *PDGFRA* gene sequences. In four patients, there was adequate tumor tissue available for mutation analysis from a surgical resection that occurred before initiation of imatinib.

Full-length KIT cDNA sequencing. For GISTs lacking a detectable *KIT/PDGFRA* mutation by genomic DNA analysis, we amplified and sequenced the complete *KIT* cDNA, to avoid false-negative results. Adequate RNA was obtained in three tumor nodules from two patients (Table 1) by using the RNA Wiz reagent (Ambion, Inc., Austin, TX) and the guanidine isothiocyanate/phenol/chloroform method. Five micrograms of RNA were transcribed using reverse transcriptase superscript II (Invitrogen, Carlsbad, CA). The cDNA was subjected to PCR using the following *KIT* primers: 1F, GATTTTCTCTGCGTTCTGCTC; 6R, GGGGAATGCTTCATATTCAACAATCAAATCTAC; 6F, GTAGATTTGATTGTTGAATATGAAGCATTCCCC; 12R, AAAGCTCCAGCACCCAGGGTTTT; 10F, TTCTGACCTACAAATATTTACAG; 16R, TGGGACAACATAAGAAACTCCAGG; 15F, GGAGATCTGTGAGAATAGGCT; 18R, CTAAAGAGAACAGCTCCCAAA; 17F, CTCATGGTCGGATCACAAAGA; 21R, GACAGAATTGATCCGCACAGA. Direct sequencing of PCR products was done for all exons tested, and each ABI sequence was compared with the National Center for Biotechnology Information human *KIT* cDNA sequences.

Immunohistochemistry. Immunohistochemical stains were done on formalin-fixed, paraffin-embedded tissue of the tumors using standard protocols. The antibodies used for the immunohistochemical stains were CD117 (DAKO, Carpinteria, CA; 1:500); Desmin (DAKO; 1:50); SMA (Novocastra, Newcastle Upon Tyne, United Kingdom; 1:50); and CMA, Ki67, p53, and Bcl2 (Ventana Medical Systems, Inc., Tucson, AZ; prediluted).

p53 *mutation analysis.* Mutation analysis was done in cases showing p53 positivity, using >20% nuclear staining as a threshold. PCR was done from 1 μg of genomic DNA extracted from frozen or macrodissected formalin-fixed, paraffin-embedded tissue. The main hotspots for *p53* mutations were screened, including exons 5 to 8. Primer sequences and annealing temperatures used are listed in Table 2.

Western blotting. Tumor whole-cell lysates were prepared from 10 nodules by grinding 1 g of snap-frozen tumor tissue, using a PowerGen 700 Homogenizer (Omni International, Marietta, GA). The ground tissue was resuspended in radioimmunoprecipitation assay lysis buffer (Upstate, Lake Placid, NY) containing a cocktail of protease and phosphatase inhibitors (Sigma, St. Louis, MO), sodium fluoride, sodium orthovanadate, and phenylmethylsulfonyl fluoride. Protein concentrations were determined using the Bio-Rad protein Assay (Bio-Rad Laboratories, Hercules, CA). Electrophoresis and immunoblotting were done on the protein extracts using the standard protocol, using 50 μg of protein per sample. Antibodies tested on the immunoblots included rabbit polyclonal anti–phospho-KIT Y721 (Zymed Lab, Inc., San Francisco, CA), rabbit anti-KIT (Oncogene Science, Boston, MA), mouse anti-actin (Santa Cruz Biotechnology, Santa Cruz, CA), anti–phospho-AKT (Thr^{308}), anti-AKT, anti–phospho p44/p42 mitogen-activated protein kinase (Thr^{202}/Tyr^{204}), anti–mitogen-activated protein kinase, anti–phospho-mammalian target of rapamycin (Ser^{2448}), anti–mammalian target of rapamycin, anti–phospho-phosphoinositide-dependent kinase 1(Ser^{241}), anti–phosphoinositide-dependent kinase 1, anti–phospho-S6 ribosomal protein ($Ser^{235/236}$), and anti–S6 ribosomal protein (Cell Signaling Technology, Inc., Danvers, MA). The secondary antibodies used included donkey-anti-mouse (Santa Cruz Biotechnology) and anti-rabbit (Calbiochem, La Jolla, CA). Following hybridization with the secondary antibody, the blots were incubated with Immun-Star horseradish peroxidase luminal/enhancer (Bio-Rad) and exposed onto Kodak Biomax MR Film (Eastman Kodak Co., Rochester, NY).

Electron microscopy. Representative fresh tumor tissue was fixed in 3% glutaraldehyde/3% formaldehyde in a 0.1 mol/L Milonigs phosphate buffer. After buffer rinse, the tissue was postfixed in 1% osmium tetroxide, dehydrated, and embedded in epoxy resin using standard procedures. In each case, thick sections were cut and stained with toluidine blue, and representative blocks were chosen for ultrastructural evaluation. Thin sections were stained with uranyl acetate followed by lead citrate and examined with a Philips EM401 electron microscope. Changes consistent with therapy effect were recorded, such as increased collagenous stroma, lysosomal structures, and lipid vacuoles.

U133A chip Affymetrix microarray analysis. Microarray analysis was done on 10 nodules from three responsive GIST patients (patients 1, 2, and 4). Cases tested on the array platform were selected amongst tumors with considerable viable tumor (grade 1 or 2 histologic response) and high levels of total KIT by Western blotting. Two of the patients had a *KIT* exon 11 mutation, and one patient had an exon 9 mutation. The expression pattern was compared with a group of 34 nontreated GISTs that were selected from our database. To match the study group, only nontreated GISTs with mutations in *KIT* exon 11 or 9 were selected for the control group. There were 27 *KIT* exon 11 and 7 *KIT* exon 9 mutated GISTs in the control group. As previously described (11), RNA was isolated using RNAwiz RNA Isolation Reagent (Ambion) followed by treatment with RNase-free DNase (Qiagen, Valencia, CA) according to the manufacturer's instructions. Twenty-five to 50 ng of total RNA was tested for quality on an RNA 6000 Nano Assay (Agilent, Palo Alto, CA) using a Bioanalyzer 2100. RNA with an A_{260}/A_{280} ratio >1.8 was chosen for expression profiling experiments. Two micrograms of high-quality total RNA were then labeled according to protocols recommended by the manufacturer. Briefly, after reverse transcription with an oligo-dT-T7 (Genset, La Jolla, CA), double-stranded cDNA was generated with the Superscript double-stranded cDNA synthesis custom kit (Invitrogen/Life Technologies, Carlsbad, CA). In an *in vitro* transcription step with T7 RNA polymerase (MessageAmp RNA kit, Ambion), the cDNA was linearly amplified and labeled with biotinylated nucleotides (Enzo Diagnostics, Farmingdale, NY). Ten micrograms of labeled and fragmented cRNA were then hybridized onto a test array and a Human Genome U133A expression array (Affymetrix, Inc., Santa Clara, CA; containing 22,000 transcripts). Post-hybridization staining and washing were processed according to the manufacturer (Affymetrix). Finally, chips were scanned with a high-numerical aperture and flying objective lens in the GS3000 scanner (Affymetrix).

Expression data analysis. The images were quantified using a GCOS1.1 (GeneChip Operating System, Affymetrix) with the default variables for the statistical algorithm and all probe set scaling with a target intensity of 500 to account for differences in the global chip intensity. The expression values were transformed using the logarithm base 2. To find genes that associated with different GIST subsets, we applied filtering and statistical analysis constraints to the expression data to exclude those genes that did not vary significantly between comparison groups (<2-fold change) or that were not expressed at high enough levels. A statistical group analysis was carried out to find genes that showed statistically significant differences in mean expression levels between the responsive and nontreated GISTs. The log of the

Table 1. Molecular and clinicopathologic features in 28 patients with imatinib-responsive GISTs

Patient	Primary mutation	Disease at start of imatinib	Duration of imatinib (mo)	Best clinical response	Histologic response	Ki67 (%)	p53 (%)	Follow-up (mo/status)
1*	Exon 11 del 569-576 VYIDPTQL	P, L	22	PR	2	0	0	20/SD
2A*†	Exon 11 P551H H-del 552-4 MY	P, Pe, L	15	PR	2	0	0	23/SD
2B	Exon 11 P551H H-del 552-4 MY	L	20	PR	1	<1	0	
3A	Exon 9	Pe	12	SD	1	10-15	10-20	24/POD
3B†	Exon 9	Pe	18	SD	1	5-20	0-20	
4*†	Exon 9	P, L	3	SD	1	<5	—	29/NED
5	WT	P	9	PR	4	0	0	46/POD
6	Exon 9	P	4	SD	2	10-15	<5	44/NED
7	Exon 11 del	P	6	PR	4	<1	—	20/NED
8†	Exon 11 K558N, ins559 Q	P	2	PR	1	0	0	40/NED
9‡	Exon 11 del 555-559 VQWKV	Pe, L	1	PR	4	0	0	31/NED
10	Exon 11 del	P	8	PR	4	0	0	10/NED
11†§	PDGFRA exon 18 D842V	Pe	5	SD	3	20	<5	21/POD
12	Exon 11 del 563-76 INGNNYVYIDPTQL	P, Pe, L	9	PR	4	0	—	23/SD
13	Exon 13 K642E	P	8	PR	2	0	0	14/NED
14	Exon 11 del 560 V	Pe	4	PR	4	10-15	0	39/DOD
15	Exon 11 Q556H,‖ del 557-559 WKV	Pe	12	PR	4	20	0	23/POD
16†	Exon 11 del 559-565 VVEEING	P, Pe, L	7	PR	2	0	—	14/SD
17†	Exon 9	P	2	PR	1	<2	—	14/NED
18	Exon 11 INS 573-587 PTQLPYDHKWEFPRN	L	9	SD	3	0	0	15/NED
19	Exon 11 del 551-3 PMY	L	14	PR	3	0	0	11/NED
20§	WT	L	8	PR	4	0	—	13/NED
21	Exon 11 del 557-8 WK	P	6	PR	3	<1	—	10/NED
22§	Exon 11 del 551-9 PMYEVQWKV	P	6	PR	4	0	0	10/NED
23§	Exon 11 V559D	Pe	7	PR	4	0	0	12/POD
24	Exon 11 del 550-4KPMYE	P, L	31	PR	4	0	—	6/NED
25	Exon 9	Pe	6	PR	3	20	0	3/SD
26	Exon 11 del 557-70 WKVVEEINGNNYVY	P, L	14	PR	4	30	80¶	4/NED
27†‡	WT	Pe	4	SD	2	5-10	20-30	10/NED
28	Exon 11 del 554-8 EVOWK	P	6	PR	3	50-70	80¶	2/NED

NOTE: The genotype of cases 1 of 14 were previously reported.
Abbreviations: del, deletion; H-del, homozygous deletion; ins, insertion; WT, wild type; P, primary tumor; Pe, peritoneal; L, liver; PR, partial response; SD, stable disease; NED, no evidence of disease; POD, progressive disease; DOD, dead of disease.
*Sample tested for gene expression.
†Sample analyzed by fluorescence *in situ* hybridization.
‡Full-length cDNA sequencing.
§Patients with pre-imatinib tissue available for genotyping.
‖Patient with secondary mutation in *KIT* exon 13 (V654A).
¶Presence of p53 mutation.

Table 2. p53 primer sequences

Exon	Primer sequence
Exon 5 forward	5′-GTTTCTTTGCTGCCGTCTTC-3′
Exon 5 reverse	5′-AATCAGTGAGGAATCAGAGG-3′
Exon 6 forward	5′-ACATGACGGAGGTTGTGAGG-3′
Exon 6 reverse	5′-TCTCATGGGGTTATAGGGAG-3′
Exon 7 forward	5′-GACAGAGCGAGATTCCATCT -3′
Exon 7 reverse	5′-GAAGAAATCGGTAAGAGGTG-3′
Exon 8 forward	5′-GGAGTAGATGGAGCCTGGTT -3′
Exon 8 reverse	5′-GATAAAAGTGAATCTGAGGC -3′

normalized expression data was analyzed using the LIMMA method from the Bioconductor package. This method uses a modified *t* statistic. To deal with the multiple testing problem, the false discovery rate (12) method was used, and the list was cutoff at a false discovery rate of 1×10^{-4}. The gene lists obtained for each individual analysis were cross-referenced against both the published literature and the gene ontology consortium database[6] using NetAffx.[7] The data were clustered using two different methods and two gene lists. For one analysis, the genes were filtered to contain only those that were scored present in at least 25% of the samples, which gave 12,092 genes. The data were then clustered using hierarchical clustering with the Pearson correlation metric and average linkage. To assess the robustness of the clustering result, bootstrap resampling was done (13). A parametric method was used to resample the data to simulate noise. This was done 1,000 times, and each replica of the data was clustered. The 1,000 trees were then combined using a majority rule algorithm (13) to give a consensus tree. Each node was scored by how many times it appeared in the 1,000 bootstrap trees.

Hierarchical clustering analysis was also done using Genespring 7.2 software. After filtering for flags and expression values, a gene list that selected for genes with significant fold changes between the groups was identified. Hierarchical clustering with the Pearson metric and centroid linkage was used. This cluster is shown for illustrative purposes to depict the distribution of expression values for genes significantly different in the two groups. The first clustering result is unbiased in its gene selection, and the separation seen is a property of the data as a whole.

Real-time PCR validation. One microgram of total RNA was reverse-transcribed using the Thermoscript Reverse Transcription-PCR system (Invitrogen) at 52°C for 1 h. Twenty nanograms of the resultant cDNA was used in a quantitative PCR reaction using an iCycler (Bio-Rad Laboratories) and predesigned Taqman ABI Gene expression Assays [Hs00231790_m1 for ets variant gene (ETV5); Hs00605839_m1 for galanin receptor 2 (GalR2); Hs00170471_m1 for glypican 3 (GPC3); Hs00224622_m1 for myosin, heavy polypeptide 11 (MYH11); Hs00162558_m1 for transgelin (TAGLN); Hs00998133_m1 for transforming growth factor-β (TGF-β)]. Primers were chosen based on their ability to span the most 3′ exon-exon junction. Amplification was carried for 40 cycles (95°C for 15 s and 60°C for 1 min). To calculate the efficiency of the PCR reaction, and to assess the sensitivity of each assay, we also did a seven-point standard curve (5, 1.7, 0.56, 0.19, 0.062, 0.021, and 0.0069 ng). Triplicate C_T values were averaged, and amounts of target were interpolated from the standard curves and normalized to hypoxanthine phosphoribosyltransferase (assay Hs99999909_m1).

Fluorescence* in situ *hybridization analysis. Fluorescence *in situ* hybridization was done in eight GIST cases, using fresh frozen touch preparations from three tumors and on formalin-fixed paraffin sections for five tumors (Table 1). Fluorescence *in situ* hybridization was done according to standard procedures. Briefly, touch preparations were fixed in 3:1 methanol/acetic acid and then pretreated with pepsin-HCl (0.007 mol/L HCl, 8 Ag/mL pepsin) at 37°C for 3 to 5 min, rinsed in PBS, fixated in 1% formaldehyde for 10 min, then rinsed, dehydrated, and air-dried. Paraffin sections were dewaxed in xylene and then microwaved in 10 mmol/L sodium citrate (pH 6-6.5) solution for 5 to 10 min, cooled to room temperature, rinsed, and dehydrated. The slides were then denatured in 70% formamide at 68°C for 2 to 4 min, quenched, dehydrated, and air-dried. The *KIT* probes used were two overlapping BAC clones: CTD- 3180G20 and RP11-722F21 (Invitrogen), labeled by nick-translation with Spectrum Green (Vysis, Abbott Laboratories, Abbot Park, IL). The PDGFRA probe used included two BAC clones that spanned about 290 kb around the gene: RP11-117E8 and RP11-231C18. A chromosome 4 centromeric probe labeled with Spectrum Orange (CEP 4, Vysis) was used as reference. The probe mix, 50 to 80 ng of each *KIT* or *PDGFRA* BAC and 2 μL Cot-1 DNA (Invitrogen), was ethanol-precipitated and resuspended in hybridization buffer. The *KIT* or *PDGFRA* probe mix was denatured at 70°C for 10 min, followed by preannealing at 37°C for 30 min. The *KIT* or *PDGFRA* probe was then combined with the denatured CEP 4 probe on the slide, coverslipped, and incubated overnight at 37°C. After standard post-hybridization washes, the slides were stained with 4′,6-diamidino-2-phenylindole and mounted in antifade (Vectashield, Vector Laboratories, Burlingame, CA). Analysis was done using a Nikon E800 epifluorescence microscope with MetaSystems Isis 3 imaging software. A minimum of 100 cells was scanned over separate regions for each slide. Image z-stacks were captured using a Zeiss Axioplan 2 motorized microscope controlled by Isis 5 software (Metasystems, Altlussheim, Germany).

Results

We identified 28 GIST patients who had a partial response or stable disease to imatinib therapy and had a surgical resection of their tumor. There were 15 males and 13 females with an age range of 31 to 84 years (mean age = 57.2 years). At the time of diagnosis, GIST tumors were confined to the primary site in 20 patients, whereas liver metastasis was seen in four patients, peritoneal metastasis in five patients, and one patient had both liver and peritoneal metastasis. At the start of imatinib therapy, 10 patients had primary disease only, 8 patients had primary disease along with metastasis to the liver and/or peritoneum, and 10 patients had only metastatic tumors to the liver and/or peritoneum. The duration of imatinib therapy ranged from 1 to 31 months (mean = 9.1 months, median = 7 months). Two patients had tumor nodules surgically resected at two different points of time after additional imatinib therapy. Twenty-two patients showed a "partial response" to imatinib, and six patients showed "stable disease."

Half of the patients had their primary tumors located in the small bowel, whereas eight patients had primary gastric GISTs, and three patients had their tumors located in the rectum or outside the intestine (pelvis, omentum, and peritoneum). Tumors ranged in size from 1.2 to 42 cm, with a mean size of 10.6 cm. The morphology of the primary tumor was spindle in 23 of the tumors and epithelioid in 5 tumors.

Follow-up data were available in all 28 patients and ranged from 2 to 46 months, with a median follow-up of 11.5 months (Table 1). Seventeen (60.7%) patients showed no evidence of disease; 5 (18%) patients had stable disease; 5 (18%) patients had progressive disease; and 1 (3.5%) patient died of the disease. Eighteen (64%) patients continued imatinib treatment at the time of the follow-up. Of the remaining 10 patients,

[6] http://www.geneontology.org/.
[7] http://www.affymetrix.com.

three patients stopped imatinib therapy after a very good response of their primary tumors. The remaining patients stopped imatinib therapy due to toxicity, progressive disease, or death.

Histologic response does not correlate with imatinib therapy duration or with proliferative activity. Twelve (43%) patients, following imatinib therapy ranging from 1 to 31 months, showed a grade 4 response to imatinib in their resected tumors, with >90% fibrosis and necrosis. A grade 3 response was seen in tumors removed from 6 (21%) patients and grade 2 response in 5 (18%) patients. Limited or no response (grade 1) was noted in 5 (18%) patients, following imatinib therapy ranging from 2 to 20 months. The degree of response did not correlate with the duration of imatinib therapy. Patient 9 had a grade 4 response after only 1 month of imatinib therapy, whereas one of the tumor nodules in patient 2 showed a grade 1 response, after 20 months on imatinib (Table 1).

The histologic response was minimal (grade 1) in two of six patients defined clinically as having stable disease and mild to moderate (grade 2-3) in the remaining four patients. More than half (54%) of the 22 patients with a clinical partial response had a very good histologic response (grade 4), whereas 3 (14%) patients had a minimal (grade 1) response, and the remaining 7 (32%) patients had a mild to moderate response.

The histologic response of GIST tumors to imatinib therapy was heterogeneous, not only from nodule to nodule within the same resection but also within the same lesion. Some tumors showed only gross tumor necrosis, with large, central areas of cystification and hemorrhage, whereas the remaining solid areas seemed viable microscopically. Only a few tumors showed dense hyalinization with a complete loss of tumor cells. Most tumors showing a grade 4 response had microscopic foci of viable cells seen either as isolated tumor cells or distinct micronodules embedded in an extensively hyalinized background (Fig. 1A). In some of the peritoneal tumor nodules, an unusual pattern of viable tumor growing along the peritoneal surface was identified (Fig. 1B). Immunostaining for KIT proved to be extremely useful in identifying and confirming residual viable tumor cells in the hyalinized areas, which could have been overlooked on histologic evaluation alone. The histologic response did not correlate with the size of the tumor. Tumors with a grade 4 histologic response ranged in size from 1.2 to 21.0 cm (mean = 9.8 cm), whereas tumors with a minimal grade 1 response ranged in size from 2.6 to 18 cm (mean = 9.0 cm).

In 21 (75%) patients, tumor sections from viable areas showed no mitotic activity in the different nodules analyzed. In the remaining seven patients, including four partially responsive and three with stable disease, the mitotic activity ranged from 10 to 100 per 50 high-power fields. Mitotic activity did not correlate with the *KIT* genotype or overall response of the tumor to imatinib therapy. Even with a grade 4 histologic response, actively mitotic viable tumor foci were identified. In some other patients with a minimal to moderate (grade 1-3) response, the tumors showed minimal to no mitotic activity even with large areas of viable tumor. The Ki67 proliferative index ranged from 0% to 70% in viable foci and consistently correlated with mitotic activity. In tumors with no mitotic activity, Ki67 showed <5% staining (Fig. 1A and C). The proliferative index, similar to mitotic activity, did not correlate with the clinical response, *KIT*/*PDGFRA* mutation type, histologic response, or the duration of imatinib therapy. Patient 3, who showed a grade 1 response, had a 20% Ki67 proliferative index after 18 months of imatinib therapy, whereas patient 26, who had a grade 4 response, showed a proliferative index of 30% after 14 months of imatinib therapy.

All of the tumor samples were KIT (CD117) positive except for one nodule (patient 19) that showed residual viable tumor. The intensity and extent of staining ranged from focal, weak staining to a diffuse strong positivity. KIT staining of tumors showed no consistent correlation with the response to imatinib. Strong KIT reactivity was typically seen in mitotically active areas (Fig. 1B), whereas a weaker staining pattern was noted in mitotically quiescent areas, even if largely viable (Fig. 1C). Furthermore, in responsive areas of the tumor with dense hyalinization and fibrosis, KIT staining highlighted isolated viable tumor cells.

Immunohistochemical staining for Bcl2 was done in 19 tumors from 19 patients. Nine tumors showed positivity for Bcl2, with a strong and diffuse pattern in four cases. Bcl2 positivity did not seem to correlate with the histologic response, mitotic activity, or the proliferative index of the tumor. The strongly Bcl2-positive tumors were associated with a variable proliferation index (0-20%) and had a wide range of histologic response (grade 1-3). Similarly, the Bcl2-negative GISTs did not correlate with either proliferation index or histologic response.

p53 immunostaining was done on 22 tumors from 20 patients, selected among tumors with high proliferative activity, and results showed low or no expression (0-20% nuclear staining) in all except three cases. Two of the latter three cases showed strong and diffuse p53 nuclear reactivity in most of the cells (>80%). These two cases had a similar phenotype, including a *KIT* exon 11 deletion, strong KIT expression, a high proliferative index >30% in the viable areas, absence of Bcl2, and either a moderate (grade 3) or good (grade 4) histologic response (Fig. 1E). The third case, which showed 20% to 30% p53 positivity, had a minor (grade 1) histologic response, strong Bcl2 reactivity, and a low mitotic activity (Table 1). In these three cases, p53 mutation analysis was done for the major hotspots, including exons 5 to 8. Both cases with >80% immunoexpression of p53 showed a single amino acid substitution in exon 5 (I162S) and exon 8 (R282W; Fig. 1E, respectively). The pre-imatinib tumor tissue was available in these two cases and showed a similar high expression of p53, immunohistochemically.

Electron microscopy identifies a subset of tumors with smooth muscle phenotype. Ultrastructural analysis was done on 16 tumors. Nine tumors were associated with minimal histologic response, and the ultrastructural changes were very subtle, with minimal increase in the collagen matrix and rare cells showing a slight increase in actin microfilaments, lysosomes, and fat droplets. However, most cells seemed unaltered and resembled the ultrastructural features of imatinib-naive GIST, with long interdigitating cell processes, skeinoid fibers, etc. The remaining seven tumors showed marked therapy-related changes ultrastructurally, with cells widely separated by a prominent extracellular collagenous matrix. In most of these tumors, the cells showed an increased number of cytoplasmic lysosomes and fat droplets (Fig. 1F). In only a few cases, the tumor cells had an inactive appearance, with high nuclear/cytoplasmic

ratio and a paucity of cytoplasmic organelles. Four cases in this group showed increased deposits of actin microfilaments, with pinocytotic vesicles and a linear basement membrane, suggestive of true smooth muscle differentiation (Fig. 1F). Two of these four tumors showed desmin immunopositivity (Fig. 1F), whereas the CD117 was weakly positive. The remaining two cases were desmin negative, but actin (SMA and/or CMA) positive. The combined ultrastructural features and

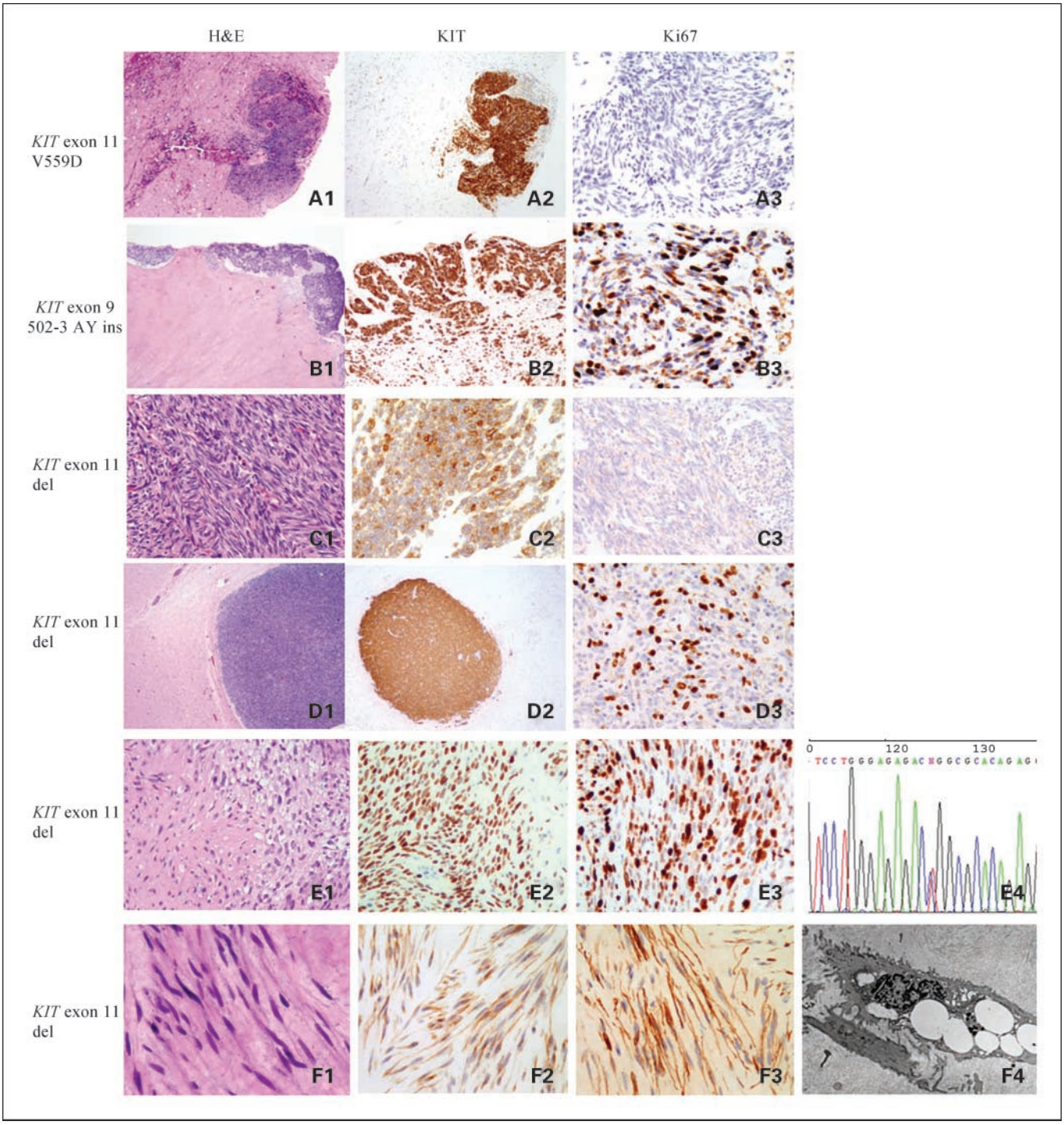

Fig. 1. Histologic response and proliferation activity in imatinib-responsive and stable GIST with (*A*), a primary *KIT* exon 11, grade 4 histologic response, and a nil Ki67 index (patient no. 23 developed POD after 12 months) (*A1*, H&E, 4×; *A2*, KIT 4×, *A3*, Ki67 20×); (*B*) *KIT* exon 9 mutation, grade 3 histologic response (80-85%), and 20% Ki67 index (patient no. 25) (*B1*, H&E 2×; B2, KIT 4×; *B3*, Ki67 20×); (*C*) *KIT* exon 11 deletion, grade 2 response (40%), lower KIT expression, and nil Ki67 (patient no. 16, with stable disease after 14 months) (*C1*, H&E 10×; *C2*, KIT 20×; *C3*, Ki67 20×); (*D*) primary *KIT* exon 11 deletion, a second-site *KIT* exon 13 V654A, grade 4 response, Ki67 of 20% (patient no. 15, NED after 17 months) (*D1*, H&E 2×; *D2*, KIT 2×; *D3*, Ki67 20×). Pathologic findings in responsive GIST showing (*E*) primary *KIT* exon 11 deletion, grade 3 response (70%), high Ki67 (50-70%) index, diffuse and strong p53 (80%) expression, and a p53 exon 8 R282W substitution (patient no. 28) (*E1*, H&E 10×; *E2*, Ki67 10×; *E3*, p53 20×; *E4*, ABI sequence); (*F*) smooth muscle differentiation by immunohistochemistry (diffuse desmin reactivity, with weaker KIT expression) as well as ultrastructurally (presence of abundant actin microfilaments arranged in dense fusiform bodies and attachment plaques, numerous pinocytotic vesicles) (patient no. 10) (*F1*, H&E 20×; *F2*, KIT 20×; *F3*, desmin 20×; *F4*, electron micrograph 9,900×).

immunoprofile suggested that at least a minority of the imatinib-treated GIST might have undergone trans-differentiation to a smooth muscle phenotype.

Second-site KIT mutations are extremely rare events in clinically responsive tumors. *KIT* and *PDGFRA* mutation analysis was done in all 48 nodules. In 18 patients (64%), a primary mutation was detected in *KIT* exon 11, which was predominantly an in-frame heterozygous deletion. Only one of the 15 cases with *KIT* exon 11 deletions showed loss of heterozygosity in some but not all nodules examined (patient 2). In one patient each, the tumors showed a *KIT* exon 11 V559D substitution, a 3′ internal tandem duplication, and a 5′ one-amino-acid insertion. Of interest, in patient 9, the presence of a primary mutation, seen in *KIT* exon 11 (del 555-559 VQWKV), was identified only after full-length cDNA sequence of *KIT* (Table 1). The initial genomic DNA PCR showed a wild-type genotype, most likely as a false-negative result due to extensive necrosis.

KIT exon 9 mutation (502-3 AY ins) was identified in 5 cases (18%), and exon 13 (K642E) was identified in 1 case (3.5%). *PDGFRA* exon 18 (D842V) mutation was seen in 1 case (3.5%), and 3 cases (10.5%) lacked mutations in *KIT* or *PDGFRA*. In all except one patient, the tumors lacked secondary mutations in *KIT* or *PDGFRA*. A second-site *KIT* exon 13 mutation (V654A) was identified in patient 15, which was present in two of three nodules tested. In fact, the tumor in this patient showed a very good (>90%) histologic response with few viable foci showing a mitotically active tumor, following 12 months of 400 mg/d imatinib treatment (Fig. 1D). Interestingly, this patient recently developed clinical progression in a 3.0-cm peritoneal nodule, 23 months subsequent to the resection of his responsive disease. Before the current surgical resection, the patient's imatinib dose was increased to 800 mg/d; however, the positron emission tomography studies showed no decrease in uptake. The pathologic exam of this nodule showed no histologic response. Genotypic analysis showed a primary *KIT* exon 11 mutation and a second site mutation in exon 14 (T670I), suggesting that this resistant nodule originated from a different clone than the responsive nodule harboring a V654A secondary mutation.

Ten (55.5%) of 18 tumors with a *KIT* exon 11 mutation had a grade 4 histologic response, with the remaining tumors showing a grade 1 to 3 response. None of the five tumors with *KIT* exon 9 mutations showed a good response, with three tumors showing a grade 1 histologic response. Interestingly, two of the three tumors with wild-type genotype showed a grade 4 histologic response.

Gene copy number alterations of KIT/PDGFRA are not identified in responsive GIST. Fluorescence *in situ* hybridization analysis was done on a total of eight tumor nodules with a poor histologic response (grades 1-2). Three of the tumors (2A, 3B, and 4) were analyzed previously for *KIT* gene copy number changes and were found normal (6). Additional five tumor samples (Table 1) were analyzed for alterations in *KIT* and *PDGFRA* copy number with reference to a centromeric probe on chromosome 4. None of the samples showed an altered *KIT/CEP4* or *PDGFRA/CEP4* ratio when compared with control samples.

Activation of KIT and downstream targets is consistent in responsive GIST. KIT activation as measured by phosphorylation by Western blotting showed no correlation with the histologic response of the tumor. KIT was phosphorylated in 8 of the 10 tumors analyzed. Two of the tumors with grade 4 histologic response lacked phosphorylated or total KIT, most likely due to extensive necrosis. All eight tumor nodules analyzed for activation of downstream effectors of KIT signaling showed phosphorylation of phosphoinositide-dependent kinase 1, AKT, mitogen-activated protein kinase, mammalian target of rapamycin, and S6 ribosomal protein (Fig. 2). The intensity of phosphorylation of KIT and the downstream effectors seemed consistent and showed no correlation with the duration of imatinib therapy of the tumors analyzed. The duration of therapy in the cases analyzed ranged from 4 to 22 months. The activation pattern of KIT and downstream effectors was compared with a group of eight nontreated GISTs. There was inconsistent KIT activation observed in the untreated control group (6), and although phospho-KIT was detected in all eight imatinib-naive tumors tested, there was weak phosphorylation in five tumors, including all four GISTs with *KIT* exon 11 in-frame deletions. The three untreated GISTs with an identical 557-8 WK deletion showed weak expression of only the mature KIT isoform. There was strong phosphorylation in the remaining three cases with *KIT* exon 11 point mutations. Similar to KIT receptor activation, the downstream effectors of KIT signaling also showed heterogeneous and inconsistent

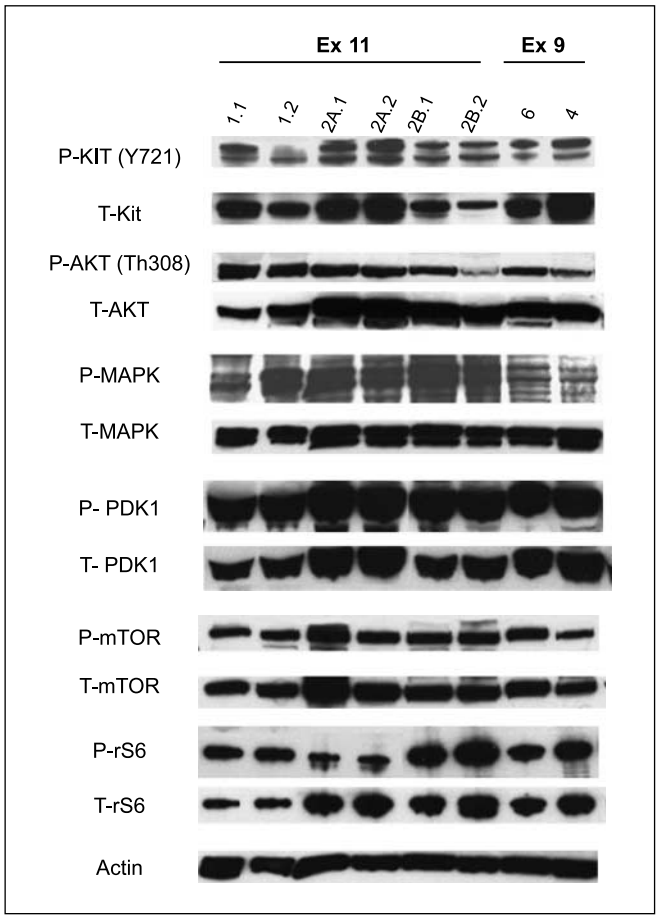

Fig. 2. Western blotting analysis done on eight tumor nodules showing activation (phosphorylation) of KIT and downstream signaling targets in responsive tumors.

phosphorylation/activation in the untreated control group (data not shown).

Genomic signature of imatinib response identifies alterations of cell cycle control and overexpression of genes involved in muscle differentiation and function. Microarray analysis done by applying a false discovery rate cutoff of 1×10^{-4} revealed a total of 230 genes to be differentially expressed between imatinib-responsive GIST and the untreated control group. The top ranked genes are listed according to their function and associated biological process in Table 3. *GalR2* and *GPC3* were the two top genes overexpressed in responsive GIST (fold change of 117 and 59, respectively).

A number of genes involved in smooth muscle contraction and development were overexpressed in the responsive GIST tumors, including *TAGLN* (a.k.a. SM22α), *LMOD1* (leiomodin 1; smooth muscle), *MCAM* (melanoma cell adhesion molecule), *MYH11* (smooth muscle), *TPM1* (tropomyosin 1), *ACTA2* (actin, α 2, smooth muscle, aorta), *CNN1* (calponin 1, smooth muscle), *DSTN* (actin depolymerizing factor), *VCL* (vinculin), *LAMA4* (laminin, α 4), etc. Of interest, all of these genes we had previously found to be differentially up-regulated in leiomyosarcoma when compared with a group of untreated GIST (14).

GALR2, *GPC3*, *TAGLN*, *MYH11* (smooth muscle), *TGFB1* (Camurati-Engelmann disease), and *ETV5* genes were validated using quantitative real-time PCR (Table 4).

Unsupervised hierarchical clustering of the two GIST subsets was done using the bootstrap analysis and simultaneously using GeneSpring version 7.2 software. The clustering analysis using both methods was identical and showed that the responsive GISTs formed a distinct cluster (Fig. 3). The only

Table 3. Differentially expressed genes in responsive versus imatinib-naive GIST

Gene symbol	Gene title	*P*	Fold change	Chromosomal location	Gene ontology biological process
Skeletal and muscular development and function					
*GALR2**	Galanin receptor 2	4.7e−13	117.48	17q25.3	Muscle contraction, G-protein–coupled receptor signaling
*TAGLN**	Transgelin	2.08e−09	20.72	11q23.2	Muscle development
LMOD1	Leiomodin 1 (smooth muscle)	9.81e−10	15.57	1q32	Muscle development
*MYH11**	Myosin, heavy polypeptide 11, smooth muscle	2.73e−08	9.91	16p13.13-p13.12	Striated muscle contraction
TPM1	Tropomyosin 1 (α)	1.32e−06	5.24	15q22.1	Muscle contraction
VCL	Vinculin	1.16e−06	2.11	10q22.1-q23	Cell adhesion
LAMA4	Laminin, α 4	4.18e−10	2.02	6q21	Cell adhesion
CNN1	Calponin 1, basic, smooth muscle	0.00068	8.72	19p13.2-p13.1	Smooth muscle contraction
ACTA2	Actin, α 2, smooth muscle, aorta	1.41e−06	4.86	10q23.3	Muscle development
PLEKHC1	Pleckstrin homology domain containing, family C (with FERM domain) member 1	0.000737	4.24	14q22.1	Actin cytoskeleton organization and biogenesis
Cellular growth and proliferation					
*GPC3**	Glypican 3	3.1e−12	59.1	Xq26.1	Extracellular matrix
*ETV5**	Ets variant gene 5 (ets-related molecule)	1.05e−11	−22.38	3q28	Transcription, DNA dependent
DUSP6	Dual specificity phosphatase 6	2.84e−07	−11.64	12q22-q23	Cell cycle
NTRK2	Neurotrophic tyrosine kinase, receptor, type 2	9.01e−05	20.73	9q22.1	Transmembrane receptor protein tyrosine kinase signaling pathway
PGF	Placental growth factor, vascular endothelial growth factor-related protein	0.000826	2.27	14q24-q31	Cell cycle, positive regulation of cell proliferation
PTEN	Phosphatase and tensin homologue (mutated in multiple advanced cancers)	0.000343	−1.80	10q23.3	Protein amino acid dephosphorylation
TOP1	Topoisomerase (DNA) I	3.19e−05	−2.66	20q12-q13.1	DNA topological change
TTF1	Transcription termination factor, RNA polymerase I	8.8e−07	2.54	9q34.13	Transcription termination
RGS2	Regulator of G-protein signaling 2, 24 kDa	0.000648	−5.99	1q31	G protein–coupled receptor protein signaling pathway
VEGF	Vascular endothelial growth factor	0.000808	−4.95	6p12	Cell cycle
Cell cycle					
*TGFB1**	Transforming growth factor, β-induced, 68 kDa	3.95e−05	−13.55	5q31	Cell adhesion
CKS2	CDC28 protein kinase regulatory subunit 2	7.03e−07	−12.72	9q22	Cyclin-dependent protein kinase activity
E2F3	E2F transcription factor 3	2.06e−05	−2.71	6p22	Cell cycle
CCND2	Cyclin D2	0.000103	−9.15	12p13	Cell cycle, cell division
CCND3	Cyclin D3	9.7e−07	−2.45	6p21	Cell cycle
SMAD1	SMAD, mothers against DPP homologue 1 (*Drosophila*)	0.000477	−2.59	4q31	Transcription, DNA dependent
SMAD3	SMAD, mothers against DPP homologue 3 (*Drosophila*)	3.16e−05	−2.82	15q22.33	Transcription, DNA dependent
CDK5	Cyclin-dependent kinase 5	5.86e−07	−3.55	7q36	Protein amino acid phosphorylation
RBP1	Retinol binding protein 1, cellular	0.000104	2.48	3q23	Transport

NOTE: Selective discriminatory genes are listed with their corresponding gene designation, molecular function, *P*, and fold change.
*Genes validated by real-time PCR.

Table 4. Validation by quantitative reverse transcription-PCR

Gene	Fold change* (reverse transcription-PCR)	Fold change* (Microarray)
GALR2	614.9	117.5
GPC3	166.8	59.2
MYH11	33.0	9.9
TAGLN	8.0	20.7
ETV5	−35.6	−22.4
TGFB1	−17.6	−9.9

*Fold change is the expression in responsive GISTs relative to that in the untreated tumors.

two treated tumors harboring a *KIT* exon 9 mutation (patient 3B) tended to cluster independently. Supervised hierarchical clustering using the differentially expressed genes between the two groups (based on a fold change of 2) confirmed the distinct clustering of the responsive cases.

Discussion

The long-term outcome of imatinib treatment for metastatic GIST has emerged from several large trials. Approximately 45% of patients with metastatic GIST have a measurable response after administration of imatinib, whereas ~30% will have at least stable disease (15). Although the 2-year survival of patients with metastatic GIST treated with imatinib approximates 72%, half of the patients develop disease progression by 2 years (3). Other investigators (1, 2), with follow-up periods between 24 and 40 weeks, have reported similar rates of progression and resistance to imatinib therapy. In only a minority of cases, patients are insensitive to the drug, a so-called primary resistance.

Most of the above studies have defined clinical response based on imaging methods using the Response Evaluation Criteria in Solid Tumors for solid tumor response to therapy. Few studies have correlated the clinical response with the pathologic response of the tumor. Scaife et al. (16) compared the radiologic and pathologic response in imatinib-treated GIST followed by surgical resection and found that computed tomography scans inaccurately predicted histologic response in 30% of patients, whereas positron emission tomography scans failed to predict a pathologic response in 64% of patients. They questioned the validity of using radiologic criteria to assess tumor response to imatinib. In the present study, a very good histologic response (grade 4) was seen in more than half of the patients with a clinical partial response, but in none of the six patients with stable disease. However, a small subset (14%) of patients with partially responsive tumors showed minimal or no histologic response (grade 1). Interestingly, more than half of the patients with *KIT* exon 11 mutation or wild-type *KIT* showed a very good response (grade 4), whereas 60% of the patients with *KIT* exon 9 mutation showed a poor response (grade 1).

The histologic response of GIST to imatinib therapy is variable and heterogeneous. Even in tumors with a very good histologic response, small foci of distinctly viable tumor, which is mitotically active, can be identified. The proliferative index, assessed by Ki67 staining in the viable tumor foci, matched the mitotic activity but did not correlate with the degree of histologic response or duration of imatinib therapy. The assessment of tumor proliferation in the areas of viable foci would be a good indicator of the aggressive nature of the residual viable tumor. Thus, performing a Ki67 immunohistochemical stain, along with KIT, is helpful in the evaluation of these responsive tumors.

Bcl2 immunoexpression has been recently evaluated as a prognostic marker in GIST. Steinert et al. (17) studied Bcl2 expression in 81 GIST tumors and reported that there is a trend towards longer progression-free survival with Bcl2 expression in GISTs subsequently treated with imatinib. In our study, Bcl2 expression in stable or partially responsive GISTs did not show any correlation with histologic response or proliferation index. Additional studies are required to be definitive on this subject.

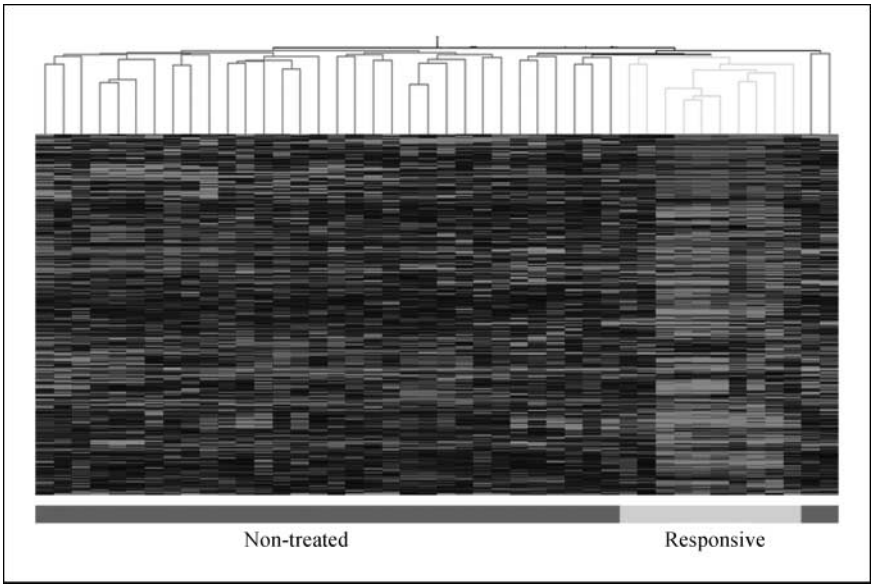

Fig. 3. Hierarchical clustering of the responsive and untreated GISTs based on 955 differentially expressed genes with a 2-fold change (Genespring 7.2).

The role of p53 alterations in GISTs remains uncertain. A few studies have suggested that p53 expression correlates with the grade and site of GISTs, being mainly gastric and high grade (18, 19). An earlier immunohistochemical study on GIST concluded that there was no role for p53 in the pathogenesis of these tumors (20). Furthermore, the role of *p53* mutations, if any, as a mechanism of developing imatinib resistance in GIST has not yet been explored. This would be relevant because *p53* mutations have been shown to be involved in the development of resistance to chemotherapy in other tumors like chronic myelogenous leukemia, lung carcinoma, breast carcinoma, hepatocellular carcinomas, etc. (21–23). Moreover, in chronic myelogenous leukemia, Bcr-Abl was shown to recruit p53 in the development of drug resistance (24). In our study, two responsive GIST tumors showed strong and diffuse overexpression of p53, both of them associated with a *KIT* exon 11 deletion, strong KIT expression, a high proliferative index >30% in the viable areas, and either a moderate (grade 3) or good (grade 4) histologic response. A single amino acid substitution was found by mutational analysis in the *p53* hotspots, exon 5 (I162S) and 8 (R282W), respectively, in these tumors. The matched pre-imatinib samples showed similar p53 expression pattern in these two cases, suggesting that the *p53* alterations through gene mutation preceded the imatinib treatment and did not affect on tumor response. Additional studies with a larger number of cases and longer follow-up are required to confirm these findings.

Second-site *KIT* mutations in the kinase domain account for half of the cases that develop secondary resistance to imatinib (6). This phenomenon seems to play a minor role in the setting of clinical response, only 1 of the 28 patients classified as clinically responsive had a second-site *KIT* mutation. Interestingly, this patient (case 15), having a primary *KIT* exon 11 deletion and a secondary *KIT* exon 13 mutation (V654A) showed a very good histologic response, with >90% fibrosis and necrosis. This patient subsequently (23 months later) developed a clinically resistant peritoneal nodule, which histologically showed no response to imatinib. Genotypic analysis of this nodule showed a *KIT* exon 11 mutation and a second-site mutation in exon 14 (T670I). This resistant nodule most likely originated from a distinct clone than the responsive nodule harboring a V654A secondary mutation.

In a prior study (6), we have investigated the status of *KIT* gene copy number in tumors by fluorescence *in situ* hybridization, including three responsive tumors. We further studied additional five cases for *KIT* and *PDGFRA* copy number changes; however, no abnormalities were identified in any tumor, with a 1:1 ratio of *KIT* or *PDGFRA* signal to the centromeric chromosome 4.

In vitro imatinib treatment of primary GIST or genetically engineered cell lines show consistent inhibition of KIT phosphorylation in the context of imatinib-sensitive mutations (25). In imatinib-naive tumor samples, the degree of activation, although present, seems less consistent and variable in pattern and intensity (6, 25). In the present study, KIT was consistently phosphorylated in most responsive tumors in which viable areas were still present. Furthermore, KIT downstream targets, such as phosphoinositide-dependent kinase 1, AKT, mammalian target of rapamycin, mitogen-activated protein kinase, and ribosomal S6, were also found to be phosphorylated. A confounding factor in our study is the cessation of imatinib 1 to 2 days before surgery. This temporary cessation of the drug before surgical resection may be responsible for the restoration of KIT phosphorylation and the biochemical activity of its downstream targets in the tumor cells. In support of this argument, activation of KIT and its signaling pathway was uniform regardless of the duration of imatinib therapy, as tumors treated in the range of 4 to 22 months showed similar phosphorylation patterns. The reactivation in KIT signaling when imatinib is discontinued before surgery is consistent with prior functional imaging observations of a "flare-up" on positron emission tomography when imatinib is interrupted, suggesting that the remaining viable but responsive tumor cells are still KIT oncogene dependent and become FDG avid. The other less likely possibility is that KIT reactivation occurs in tumors classified as clinically responsive to imatinib, and these clones are potentially resistant or in the process of acquiring resistance to the drug, either through acquisition of a secondary mutation or by other means.

An interesting observation noted by immunohistochemistry and electron microscopy was the presence of well-differentiated smooth muscle features in a subset of responsive GISTs. These tumors expressed desmin or other muscle markers along with weak positivity for KIT, which correlated with increased actin microfilaments ultrastructurally, arranged in well-defined attachment plaques and fusiform dense bodies. Furthermore, microarray analysis of responsive tumors showed a striking overexpression of the genes involved in muscle development and function, when compared with that of the nontreated tumors. These findings suggest that imatinib may induce a trans-differentiation towards a smooth muscle phenotype, through chronic inactivation of KIT signaling. A similar phenomenon was described after neutralizing interstitial cells of Cajal in mice for 8 days after birth with an anti-KIT monoclonal antibody (ACK2; ref. 26). In this setting, the interstitial cells of Cajal underwent apoptosis, and the remaining KIT immunopositive cells developed ultrastructural features similar to smooth muscle cells (26). Also overexpressed were the genes involved in the reorganization of the cytoskeleton by the interactions with actin. Thus, control of cell migration via the actin cytoskeleton provides the possibility of regulating cancer cell invasion and metastasis.

High level expression of GalR2 was found in the imatinib-responsive tumors compared with untreated GISTs. Overexpression of GalR2 has been shown to inhibit cell proliferation and induce apoptosis in neuroblastoma cell lines by activation of caspase-3 (27). Induction of receptor expression and treatment with 100 nmol/L galanin resulted in a dramatic decrease in cell viability in human SH-SY5Y neuroblastoma cells transfected with GalR2 (27). Another highly overexpressed gene in the treated subset was *GPC3*, which belongs to a family of heparan sulfate proteoglycans, that are bound to the cell surface by a lipid anchor and act as regulators of various cytokines, Wnts, Hedgehogs, etc. GPC3 expression is limited to the fetal mesodermal tissue and is known to interact with several growth factors, like fibroblast growth factor (*FGF2*) and bone morphogenetic protein-7 (*BMP-7*), thereby modulating their function (28). Increased GPC3 expression has been noted in primitive embryonal tumors, such as neuroblastomas,

Wilms' tumor, and rhabdomyosarcomas (29, 30). GPC3 was recently found to be highly expressed in hepatocellular carcinomas and was proposed as a diagnostic marker for this tumor (31). However, up-regulation of GPC3 in neoplastic tissues seems contradictory and tissue specific, inducing apoptosis in breast or ovary and oncofetal protein in liver and colon.

Furthermore, cell cycle regulators were down-regulated in the responsive group, including cyclin D2, cyclin D3, cyclin-dependent kinase 5, E2F3, ETV5, and TGF-β. The cyclin D proteins interact with the cyclin dependent kinases, leading to the phosphorylation of the retinoblastoma protein and E2F-mediated transcription and DNA synthesis. Cyclins D2 and D3 were down-regulated in the responsive tumors along with the transcription factor E2F3, as a result of imatinib therapy. Similar gene expression findings were found by our group in short-term imatinib treatment of a $KIT^{V558\Delta/+}$ mouse model of GIST (32). TGF-β pathway is an important regulatory pathway that is inhibited by imatinib, primarily due to the inhibition of PDGFR (33). The key targets of this pathway, TGF-β1, Smad 2/3, and Smad 1/5, were down-regulated in the imatinib-treated tumors.

None of the pathologic or molecular factors analyzed in this study were able to predict the clinical outcome following surgical removal of stable or responsive disease. Thus, the four patients who developed progressive disease at the last follow-up each had a different primary genotype: *KIT* exon 11, *KIT* exon 9, *PDGFRA* exon 18, and wild type. The proliferation index as determined by Ki67 immunohistochemistry in these cases ranged from 0% to 20%, and p53 staining was negative. The only patient in this series who died of disease had a grade 4 histologic response of the tumor at the time of initial surgery, following which he developed multiple recurrences at 4 and 29 months. He continued with imatinib after the recurrences were surgically removed. He was taken off imatinib, due to drug toxicity, about 3 months before his third recurrence. This patient had a *KIT* exon 11 mutation, and the Ki67 proliferation index at the time of original resection was 10% to 15%.

In conclusion, the histologic response to imatinib is heterogeneous and does not correlate well with the clinical response. The clinical outcome in stable or partial responsive GIST patients does not seem to be influenced by either the duration of the imatinib treatment, the histologic response, or the size of the tumor. Second-site *KIT* mutations are rare in GISTs responsive to imatinib compared with imatinib-resistant tumors, which harbor *KIT* kinase domain mutations in half of the cases. Chronic inhibition of KIT signaling by imatinib may induce tumor cells trans-differentiation into a smooth muscle phenotype, in a subset of cases, as suggested by the ultrastructural findings and microarray studies. Lastly, we speculate that the presence of *p53* gene alterations in GIST does not seem to affect clinical and histologic response to imatinib.

Acknowledgments

We thank Agnes Viale and Genomic Core Lab for technical assistance, Ann Baren for ultrastructural examination, and Allyne Manzo for photographic assistance.

References

1. Demetri GD, von Mehren M, Blanke CD, et al. Efficacy and safety of imatinib mesylate in advanced gastrointestinal stromal tumors. N Engl J Med 2002; 347:472–80.
2. van Oosterom AT, Judson IR, Verweij J, et al. Update of phase I study of imatinib (STI571) in advanced soft tissue sarcomas and gastrointestinal stromal tumors: a report of the EORTC Soft Tissue and Bone Sarcoma Group. Eur J Cancer 2002;38 Suppl 5:S83–7.
3. Verweij J, Casali PG, Zalcberg J, et al. Progression-free survival in gastrointestinal stromal tumours with high-dose imatinib: randomised trial. Lancet 2004; 364:1127–34.
4. Heinrich MC, Corless CL, Demetri GD, et al. Kinase mutations and imatinib response in patients with metastatic gastrointestinal stromal tumor. J Clin Oncol 2003;21:4342–9.
5. Heinrich MC, Shoemaker JS, Corless CL, et al. Correlation of target kinase genotype with clinical activity of imatinib mesylate (IM) in patients with metastatic GI stromal tumors (GISTs) expressing KIT (KIT^+). J Clin Oncol (Meeting Abstracts) 2005;23:7.
6. Antonescu CR, Besmer P, GuoT, et al. Acquired resistance to imatinib in gastrointestinal stromal tumor occurs through secondary gene mutation. Clin Cancer Res 2005;11:4182–90.
7. Therasse, Le C, Van G, et al. RECIST vs. WHO: prospective comparison of response criteria in an EORTC phase II clinical trial investigating ET-743 in advanced soft tissue sarcoma. Eur J Cancer 2005;41:1426–30.
8. Choi H. Critical issues in response evaluation on computed tomography: lessons from the gastrointestinal stromal tumor model. Curr Oncol Rep 2005;7: 307–11.
9. Van Glabbeke M, Verweij J, Casali PG, et al. Initial and late resistance to imatinib in advanced gastrointestinal stromal tumors are predicted by different prognostic factors: a European Organisation for Research and Treatment of Cancer-Italian Sarcoma Group-Australasian Gastrointestinal Trials Group study. J Clin Oncol 2005;23:5795–804.
10. Antonescu CR, Sommer G, Sarran L, et al. Association of KIT exon 9 mutations with nongastric primary site and aggressive behavior: KIT mutation analysis and clinical correlates of 120 gastrointestinal stromal tumors. Clin Cancer Res 2003;9:3329–37.
11. Antonescu CR, Viale A, Sarran L, et al. Gene expression in gastrointestinal stromal tumors is distinguished by KIT genotype and anatomic site. Clin Cancer Res 2004;10:3282–90.
12. Benjamini YHY. Controlling the false discovery rate: A practical and powerful approach to multiple testing. J Royal Stat Soc Series B Methodological 1995;57: 289–300.
13. Felsenstein J. Confidence limits on phylogenies: an approach using the bootstrap. Evolution 1985;39: 783–91.
14. Segal NH, Pavlidis P, Antonescu CR, et al. Classification and subtype prediction of adult soft tissue sarcoma by functional genomics. Am J Pathol 2003; 163:691–700.
15. van der Zwan SM, DeMatteo RP. Gastrointestinal stromal tumor: 5 years later. Cancer 2005;104: 1781–8.
16. Scaife CL, Hunt KK, Patel SR, et al. Is there a role for surgery in patients with "unresectable" $cKIT^+$ gastrointestinal stromal tumors treated with imatinib mesylate? Am J Surg 2003;186:665–9.
17. Steinert DM, Oyarzo M, Wang X, et al. Expression of Bcl-2 in gastrointestinal stromal tumors: correlation with progression-free survival in 81 patients treated with imatinib mesylate. Cancer 2006;106: 1617–23.
18. Feakins RM. The expression of p53 and bcl-2 in gastrointestinal stromal tumours is associated with anatomical site, and p53 expression is associated with grade and clinical outcome. Histopathology 2005;46: 270–9.
19. Wong NA, Young R, Malcomson RD, et al. Prognostic indicators for gastrointestinal stromal tumours: a clinicopathological and immunohistochemical study of 108 resected cases of the stomach. Histopathology 2003;43:118–26.
20. Cunningham RE, Abbondanzo SL, Chu WS, et al. Apoptosis, bcl-2 expression, and p53 expression in gastrointestinal stromal/smooth muscle tumors. Appl Immunohistochem Mol Morphol 2001;9:19–23.
21. Cavalcanti GB, Jr., da Cunha Vasconcelos F, Pinto de Faria G, et al. Coexpression of p53 protein and MDR functional phenotype in leukemias: the predominant association in chronic myeloid leukemia. Cytometry B Clin Cytom 2004;61:1–8.
22. Rahko E, Blanco G, Soini Y, et al. A mutant TP53 gene status is associated with a poor prognosis and anthracycline-resistance in breast cancer patients. Eur J Cancer 2003;39:447–53.
23. Zhou CZ, Li Y, Xu J. [Correlation between p53 gene mutation and the expression of tumor drug resistance genes in lung cancer and its clinical significance]. Zhonghua Jie He He Hu Xi Za Zhi 2004;27: 678–82.
24. Stoklosa T, Slupianek A, Datta M, et al. BCR/ABL recruits p53 tumor suppressor protein to induce drug resistance. Cell Cycle 2004;3:1463–72.
25. Duensing A, Medeiros F, McConarty B, et al.

Mechanisms of oncogenic KIT signal transduction in primary gastrointestinal stromal tumors (GISTs). Oncogene 2004;23:3999–4006.

26. Torihashi S, Nishi K, Tokutomi Y, et al. Blockade of kit signaling induces transdifferentiation of interstitial cells of Cajal to a smooth muscle phenotype. Gastroenterology 1999;117:140–8.

27. Berger A, Lang R, Moritz K, et al. Galanin receptor subtype GalR2 mediates apoptosis in SH-SY5Y neuroblastoma cells. Endocrinology 2004;145:500–7.

28. Midorikawa Y, Ishikawa S, Iwanari H, et al. Glypican-3, overexpressed in hepatocellular carcinoma, modulates FGF2 and BMP-7 signaling. Int J Cancer 2003; 103:455–65.

29. Baer C, Nees M, Breit S, et al. Profiling and functional annotation of mRNA gene expression in pediatric rhabdomyosarcoma and Ewing's sarcoma. Int J Cancer 2004;110:687–94.

30. Saikali Z, Sinnett D. Expression of glypican 3 (GPC3) in embryonal tumors. Int J Cancer 2000;89: 418–22.

31. Yamauchi N, Watanabe A, Hishinuma M, et al. The glypican 3 oncofetal protein is a promising diagnostic marker for hepatocellular carcinoma. Mod Pathol 2005;18:1591–8.

32. Rossi F, Ehlers I, Agosti V, et al. Oncogenic KIT signaling and therapeutic intervention in a mouse model of gastrointestinal stromal tumor. Proc Natl Acad Sci U S A 2006;103:12843–8.

33. Matsuyama S, Iwadate M, Kondo M, et al. SB-431542 and Gleevec inhibit transforming growth factor-beta-induced proliferation of human osteosarcoma cells. Cancer Res 2003;63:7791–8.